634 Journal of Electrical Engineering & Technology Vol. 6, No. 5, pp. 634~639, 2011
http://dx.doi.org/10.5370/JEET.2011.6.5.634

Magnetic Saturation Effect on the Rotor Core of Synchronous Reluctance Motor

Ki-Chan Kim†

Abstract – This paper presents a study on the design parameters that consider the magnetic saturation effect in a rotor core of a synchronous reluctance motor. Two important design parameters in a rotor are selected to analyze the saturation effect of a synchronous reluctance motor, particularly in a rotor core. The thickness of the main segment, which is the main path of the d-axis flux, and the end rip, which affects the q-axis flux, are analyzed using the d-axis and q-axis inductances. Moreover, the characteristics of torque and torque ripple when magnetic saturation takes place are analyzed. The saturation effect is verified by comparing the reluctance torque between the experiment and FEM simulation.

Keywords: Synchronous reluctance motor, Barrier design, D-axis and q-axis inductance, Reluctance torque

1. Introduction

The synchronous reluctance motor (SynRM) has the following advantages: cost-efficient, has high-speed capacity, and is durable to temperature. The main source of the driving force of SynRM is the reluctance torque. Thus, it is very important to design the optimal barrier and segment structure in a rotor, which is related with the d-axis and q-axis inductances for high torque density [1]-[3]. A previous work reported a new optimal design method of SynRM for the high torque and power factor using the simulation design of experiments (DOE) [4]. When performing the optimal design of the SynRM, there are several design variables related to the shape of a stator and rotor [5]. However, to decrease the simulation times as much as possible, minimum design factors are generally selected for the optimal design. Therefore, there is a need to study the design parameters that considers some factors in order to achieve the best performance after the optimal design process.

In the present paper, the reluctance torque and torque ripple characteristics that consider the magnetic saturation effect in a core are analyzed by calculating the d-axis and q-axis inductances. The thickness parameter of the main d-axis segment in a rotor is selected for the analysis of characteristics due to the d-axis magnetic saturation. The parameter of the q-axis end rip is selected for the characteristics due to the q-axis magnetic saturation. The basic model for the comparison has the optimal barriers and segments for high torque and power factor using the simulation DOE. Then, the reluctance torque and torque ripple characteristics due to magnetic saturation in a rotor core is analyzed using two design parameters based on the basis design model. Finally, the reluctance torque is verified by comparing the experiment and FEM simulation results of the d-axis and q-axis inductances of the proto basis model.

† Corresponding Author: Department of Electrical Engineering, Hanbat National University, Korea. (kckim@hanbat.ac.kr)
Received: August 24, 2010; Accepted: April 11, 2011

2. Analysis Model

To analyze the magnetic saturation effect based on the two design parameters, the basis model with high torque and power factor is designed using the optimal design process of the simulation DOE. The reluctance torque of SynRM mainly consists of the d-axis and q-axis inductances as follows [6]:

$$T = \frac{3}{2}\frac{P}{2}\left(L_d - L_q\right) i_d i_q \,. \tag{1}$$

The basic model of the optimal design process is shown in Fig. 1, and its specifications are shown in Table 1. The figure shows that the middle segment for the d-axis magnetic flux path is the main d-axis segment, and the middle rip placed on the q-axis corresponds to the end rip. The basic model has a very thin main d-axis segment and has no end rib.

The design specifications are derived from the optimal barrier and segment structures at a rated point of continuous operation. Moreover, the magnetic flux density in the segment is constrained under the saturation flux density level at the optimal design process. However, the SynRM can be used with an intermittent operating current above the rated current, which is frequently 10.5 A.

Therefore, to increase the performance at an intermittent range, we need to know the design factors that consider the magnetic saturation in a core.

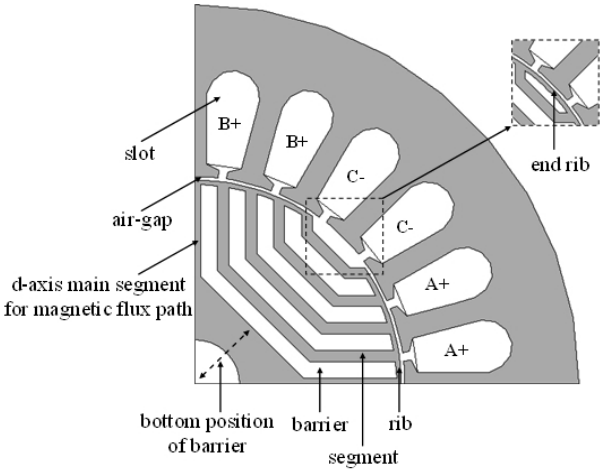

Fig. 1. Basic model for the analysis

Table 1. Specifications of the design model

Objective Specifications		
Item	UNIT	Specification
Rated Power	W	60
Battery Voltage	V_{dc}	12
Rated Current	A	10.5
Power Factor		0.73
Rated Torque/Speed	Nm/rpm	0.55/1000
Frame Size	Mm	90φ x 80

Design Specifications			
	Item	UNIT	Spec.
Rotor Design	Rib thickness	mm	0.3
	The number of barriers		5
	The bottom position of barrier	mm	9
	Flux density in the segment	T	1.4
	Air-gap	Mm	0.4
	Ratio of barrier to segment		3:2
Winding Design	Conductors per slot		44
	Coil Diameter	mm	0.75
	Voltage	V	4.78
	Power factor		0.72
	Torque	Nm	0.549
	Output Power	W	57.45
	Efficiency	%	53.04

Fig. 2 shows the flux density distributions of the basis model with 20 A input current, which correspond to the intermittent range according to the d-axis and q-axis positions of the rotor. In the case of the d-axis position, segments in the rotor are saturated because of the high input current. On the other hand, the rib is not yet saturated completely. In the case of the q-axis position, the rib is saturated and the segments are not saturated at all, which is contrary to the d-axis position. Therefore, the design parameters concerning magnetic saturation that are related to the segments and ribs should be selected.

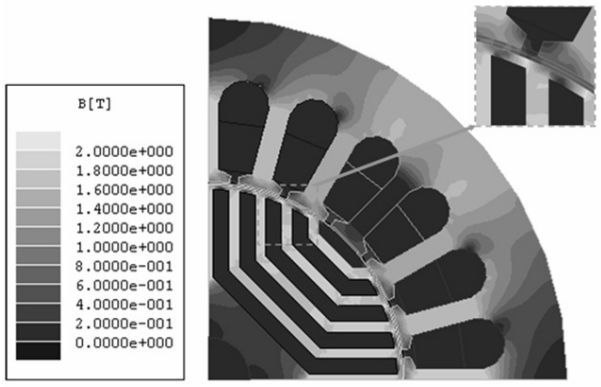

(a) d-axis positon

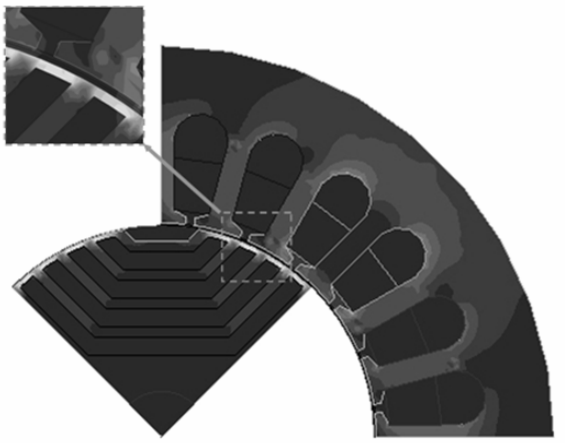

(b) q-axis position

Fig. 2. Flux density of the basis model at 20 A input current.

3. The Characteristics of the Main D-Axis Segment Parameter

First, we study the torque characteristics according to the thickness of the main d-axis segment upon considering magnetic saturation.

3.1 Comparison Models

Fig. 3 shows the comparison models for the characteristics by changing the main d-axis segment. Model 1 has the largest width of the main d-axis segment by eliminating the bottom barrier of the basis model, whereas Model 2 has a narrow barrier in the main d-axis segment.

3.2 Analysis Results

Inductance refers to the ratio of linkage flux to coil current. The d-axis and q-axis inductances are also saturated, because the magnetic flux in the core is saturated above the large current. Therefore, the reluctance torque is

not in proportion to input current from (1). We calculated the reluctance torque from the d-axis and q-axis inductance analysis according to several input currents.

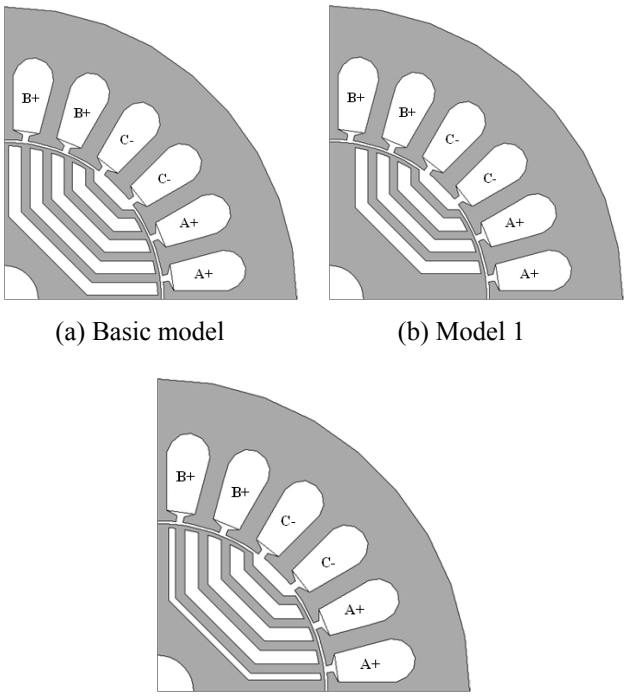

(a) Basic model (b) Model 1

(c) Model 2

Fig. 3. Comparison models considering the width of the d-axis main segment

The d-axis and q-axis inductances are calculated by 2D FEM. The method for inductance calculation is as follows. First, we inputted the three-phase current sources with instant current value at the maximum current of phase A. Next, we rotated a rotor object with constant speed. Finally, we calculated the linkage flux at each phase, which was winding with the magnetic vector potential. Fig. 4 shows the results of the analysis. We can calculate the d-axis and q-axis inductances using (2) and (3) given by:

$$L_d = \frac{3}{2} L_{aa\_\max} = \frac{3}{2} \frac{\lambda_{aa\_\max}}{I}, \quad (2)$$

$$L_q = \frac{3}{2} L_{aa\_\min} = \frac{3}{2} \frac{\lambda_{aa\_\min}}{I}, \quad (3)$$

where I is the input current for inductance calculation.

Fig. 5 shows the results of the d-axis and q-axis inductance calculations according to the input current. In the case of the q-axis inductance, each model has a uniform diminution, which is in line with the input current. However, in the case of the d-axis inductance, its basis model decreased rapidly than Models 1 and 2 because of the narrow main d-axis segment. Fig. 6 shows the magnetic flux density of Models 1 and 2 when the input current is 20 A. Comparing these with those shown in Fig. 2(a), we can see that the basis model is easily saturated than the others in the main d-axis segment, indicating that the small main d-axis segment is rapidly saturated in the core and has a bad influence on the d-axis inductance. On the other hand, Model 1 has the problem of a large q-axis inductance because of a decrease in barrier thickness.

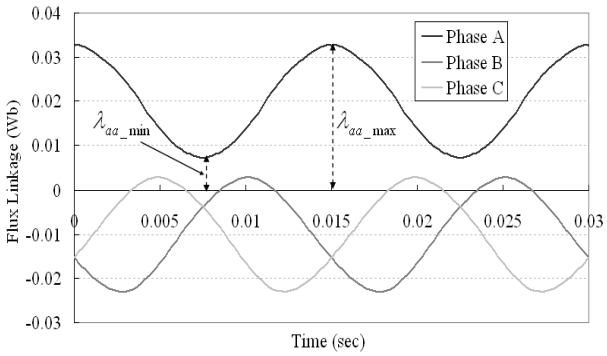

Fig. 4. The FEM analysis result after calculating L_d and L_q.

Fig. 7 shows that the maximum torque with a load angle of 45 degrees. In the case of the unsaturated level with a low input current, the reluctance torque of the basis model is higher than the others. However, Model 2 has the best torque performance when entering the saturated level. In comparison, the reluctance torque of Model 1 becomes similar to that of the basis model at the high input current region. Moreover, the torque ripple calculated by peak-to-peak value is affected by the width of the main d-axis segment and input current separately. Fig. 8 shows the comparison results of the torque ripple according to the input current. In summary, the rotor must sufficiently secure the main d-axis segment within the scope of a suitable low q-inductance.

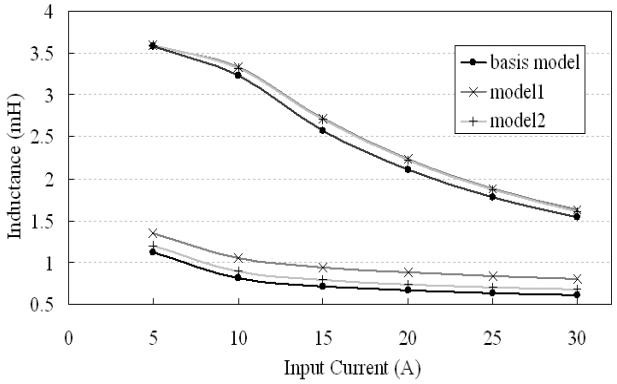

Fig. 5. Comparison of the d-axis and q-axis inductances by the main d-axis segment

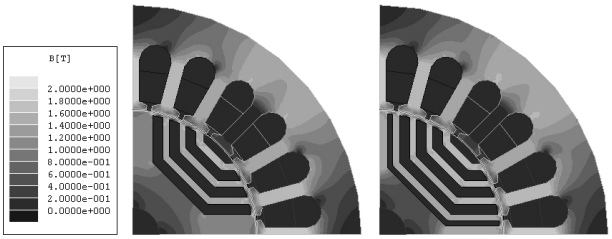

(a) Model 1 (b) Model 2

Fig. 6. Flux density at the d-axis rotor position

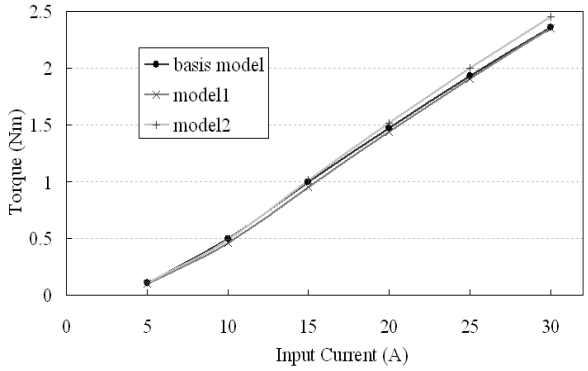

Fig. 7. Comparison of the reluctance torque according to the input current

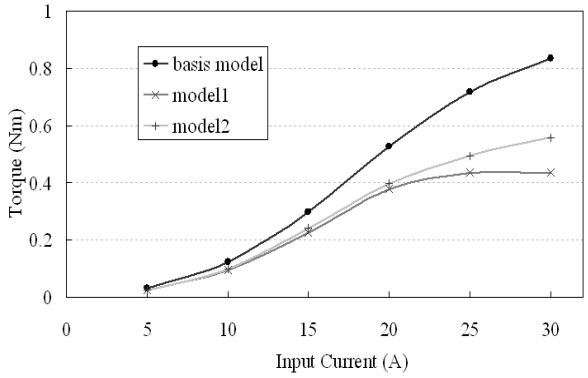

Fig. 8. Comparison of the torque ripple

4. The Characteristics of the Q-Axis End Rib

Rib refers to the main magnetic flux path at the q-axis rotor position and is generally saturated because of the narrow width. The width of the rib of the analysis models was determined as 0.3 mm by optimum design.

The second parameter study concerning magnetic saturation effect aims to analyze the torque characteristics according to the input current with a q-axis end rib parameter.

4.1 Comparison Models

The rotor with end rib may be good for mechanical noise; however, it has a higher manufacturing cost. Fig. 9 shows the models for the comparison of magnetic saturation effect according to the existence of the q-axis end rib.

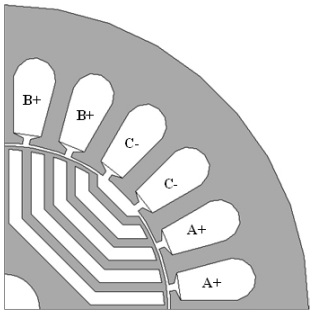

(a) Basic model

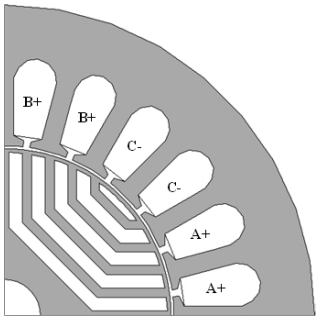

(b) Model 3

Fig. 9. Comparison models for the magnetic saturation by the q-axis end rib

4.2 Analysis Results

The d-axis and q-axis inductances of the basis model and Model 3 are calculated, as shown in Fig. 10. The d-axis and q-axis inductances of the two models decreased simultaneously according to the input current. In the case of Model 3, the d-axis inductance is slightly increased because the end rib is operated as the d-axis magnetic flux path. Meanwhile, the q-axis inductance also increased. Fig. 11 shows the saturation level of the end rib at a high input current.

Fig. 12 shows the maximum torque with a load angle of 45 degrees. We can see that the torque of both models increased similarly according to the input current. However, Fig. 13 shows that the torque ripple of the basic model is larger than that of Model 3 at the saturation level. In conclusion, the magnetic saturation of the q-axis end rib does not have an influence on the torque parameter and only decreased the torque ripple by about 4.8%. Moreover, the SynRM with an end rib has more advantages, such as possessing the mechanical strength of a rotor and having low noise and vibration.

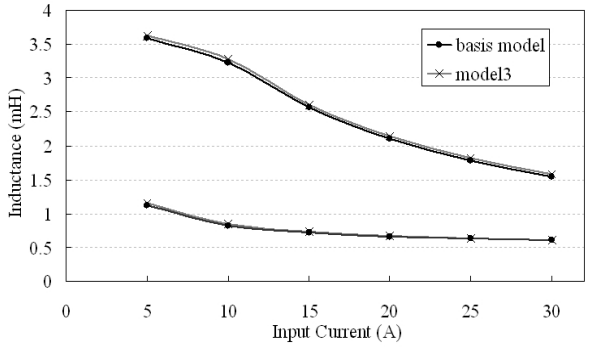

Fig. 10. Comparison of the d-axis and q-axis inductance by the q-axis end rib

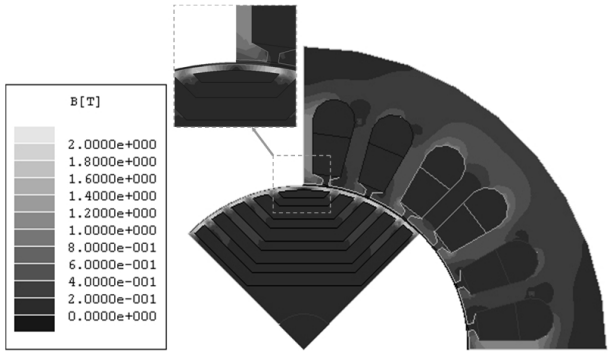

Fig. 11. Flux density at the q-axis rotor position

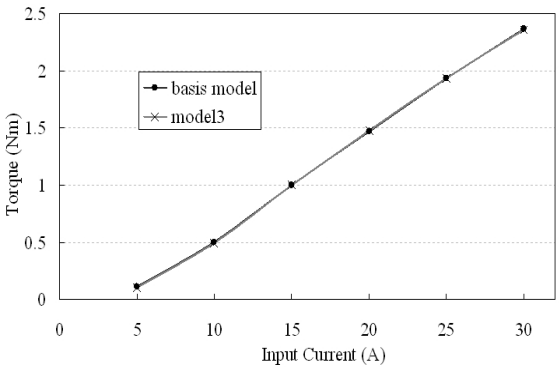

Fig. 12. Comparison of the reluctance torque according to the input current

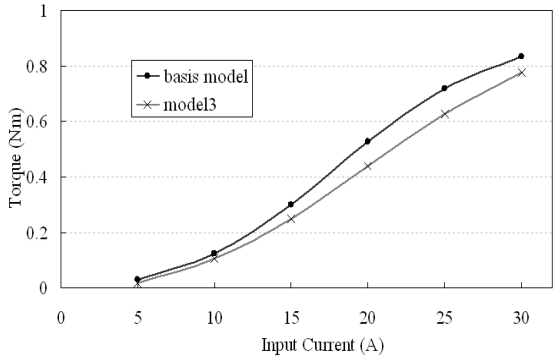

Fig. 13. Comparison of the torque ripple

5. Experimental Results

To verify the torque performance of SynRM due to design parameters, we constructed an experimental set, which consists of the dynamometer, torque sensor, SynRM, and vector inverters (Fig. 14). There is slight variation between the models in the case of the design parameter of the q-axis end rib. Therefore, we performed the experiment on torque performance in the case of the design parameter of the main d-axis segment. Fig. 15 shows the silicon steels of Models 1 and 2 for the manufactured rotor.

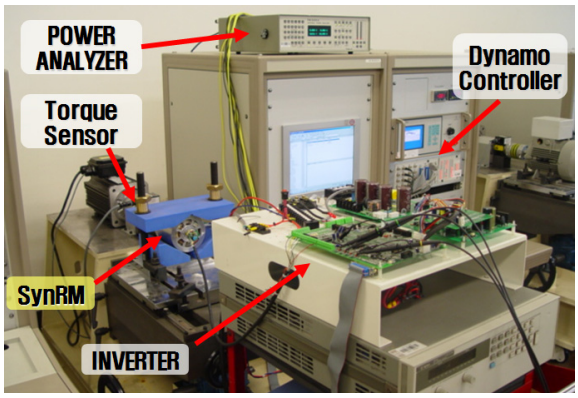

Fig. 14. Experimental set of SynRM

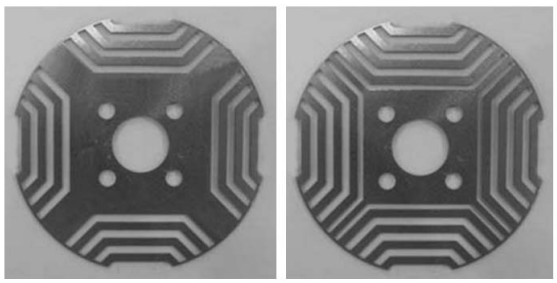

(a) Model 1 (b) Model 2

Fig. 15. Rotor cores of the proto-type SynRM

Fig. 16 shows the experimental results on the torque property of Models 1 and 2 during the operation with a 30 A input current. Similar to the simulation results shown in Figs. 7 and 8, the torque ripple of Model 1 is much smaller than that of Model 2. On the contrary, the average torque of Model 1 is similar with that of Model 2. However, the average torque by experiment is slightly higher than that of the simulation. This is because it is difficult to consider the exact B-H curve of the silicon steel in the area of deep saturation.

6. Conclusion

This paper presents a study on two design parameters, namely, the main d-axis segment and q-axis end rip, that consider the magnetic saturation effect on the rotor core.

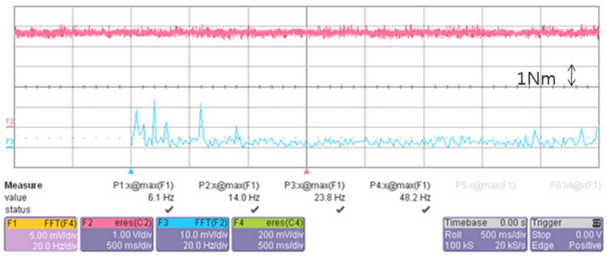

(a) Torque waveform in the case of Model 1

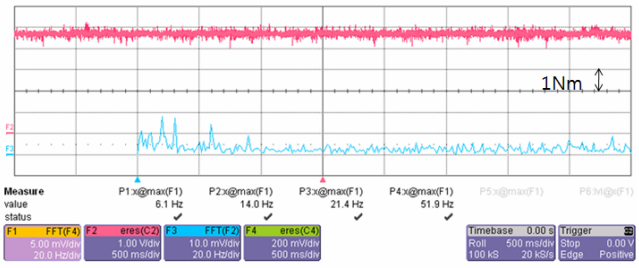

(b) Torque waveform in the case of Model 2

Fig. 16. Experimental results on the torque performance according to the thickness of the main d-axis segment at 30 A input current

The torque and torque ripple have been analyzed by the design parameters. The SynRM rotor must sufficiently secure the main d-axis segment within the scope of a suitable low q-inductance. We also verified that the magnetic saturation of the q-axis end rib does not have any influence on the torque parameter. Instead, it only reduces the torque ripple.

Acknowledgments

This research was supported by the Basic Science Research Program through the National Research Foundation of Korea (NRF), and is funded by the Ministry of Education, Science and Technology (No. 2011-0013272)

References

[1] M. Sanada, K. Hiramotor, S. Morimoto, and Y. Takeda, "Torque ripple improvement for synchronous reluctance motor using an asymmetric flux barrier arrangement", *IEEE Tran. Ind. Applicat.*, vol. 40, issue 4, pp. 1076−1082, 2004.

[2] N. Bianchi, S. Bolognani, D. Bon, and M. Dai Pre, "Rotor Flux-Barrier Design for Torque Ripple Reduction in Synchronous Reluctance and PM-Assisted Synchronous Reluctance Motors", *IEEE Tran. Ind. Applicat.*, vol. 45, issue 3, pp. 921−928, 2009.

[3] E. S. Obe, "Calculation of Inductances and Torque of an Axially Laminated Synchronous Reluctance Motor", *IET, Electric Power Application*, Vol. 4, Issue 9, pp. 783−792, 2010.

[4] K.C. Kim, J. S. Ahn, S. H. Won, J. P. Hong and J. Lee, "A Study on the Optimal Design of SynRM for the High Torque and Power Factor", *IEEE Tran. Magnetics*, vol. 43, issue 6, pp. 2543−2545, 2007.

[5] A. Vagati, T. A. Lipo, I. Boldea, T. Fukao, L. Malesani, and T. J. E. Miller, Synchronous Reluctance Motors and Drives A New Alternative, *IEEE Industru Applications Society 29th Annual Meeting*, Section 3, 1994.

[6] Matsuo, T. and Lipo, T.A., "Rotor design optimization of synchronous reluctance machine", *IEEE Tran. Energy Conversion,* vol. 9, issue. 2, pp. 359−365, June 1994.

Ki-Chan Kim was born in Korea on August 8, 1972. He received his B.S., M.S., and Ph.D. degrees in Electrical Engineering from Hanyang University, Seoul, Korea in 1996, 1998 and 2005, respectively. He worked for Hyundai Heavy Industries Co., Ltd. from 1998 to 2005. Currently, he is an Assistant Professor in Electrical Engineering at Hanbat National University, Daejeon, Korea. His special area of interest includes the design and analysis of electrical rotating machine and sensors for electric vehicles.